

## Development of the Electrochemical Imaging Technology for Visualizing Catalytic Active Site

触媒活性サイトの電気化学イメージング技術の開発

TAKAHASHI Yasufumi

高橋 康史

To develop high-performance catalysts, it is important to understand the relationship between the micro/nanoscale structures of catalysts and catalytic activity. Catalytic reactions progress in multiple steps, such as diffusion, adsorption, and dissociation of molecules in solution. Therefore, local operando measurement technology in liquid is indispensable for visualizing catalytic active sites. To visualize the catalytic active site, a nanopipette filled with electrolyte is used to form a nanoscale electrochemical cell on the sample by developing scanning electrochemical cell microscopy (SECCM). Using this technique, we visualized the catalytically active sites of MoS<sub>2</sub> nanosheets, which are expected to catalyze the hydrogen evolution reaction.

高性能な触媒を開発するうえで、触媒のマイクロ・ナノスケールの構造と触媒活性の関係を理解することは重要である。触媒反応では、溶液中での分子の拡散・吸着・解離など、マルチステップで反応が進行するため、触媒活性サイトを可視化するには、液中での局所的なオペランド計測技術が不可欠である。そこで、電解液を充填したナノピペットを用いてサンプル上にナノスケールの電気化学セルを形成する。さらに走査型プローブ顕微鏡技術を応用することで、試料表面の触媒活性サイトを可視化する走査型電気化学セル顕微鏡(SECCM)を開発した。この手法を用いて、水素生成の触媒として期待されるMoS<sub>2</sub>ナノシートの触媒活性サイトを可視化した。

### Introduction

To slow global warming, reducing CO<sub>2</sub> emissions is essential. Among them, electrochemical hydrogen evolution reaction (HER) is one of the key technologies to produce hydrogen known as a clean energy source. Platinum (Pt) is the catalyst that can efficiently generate hydrogen. Since the price of Pt is high, the development of a catalyst to replace Pt is desired.

Two-dimensional (2D) layered transitional metal dichalcogenides<sup>\*1</sup>, molybdenum disulfide (MoS<sub>2</sub>) is one of the most promising precious rare metal-free catalysts for HER.<sup>[1]</sup> To improve the catalytic activity of MoS<sub>2</sub>, significant efforts have been made in terms of conductivity improvement, chemical doping, phase transition, strain, and defect engineering.<sup>[2]</sup> Quantitatively identifying and

characterizing catalytically active sites in MoS<sub>2</sub> are critically important for understanding the catalysis of MoS<sub>2</sub>. However, it is still difficult to directly visualize the HER activity site on MoS<sub>2</sub> nanosheets. Therefore, it is necessary to develop a measurement technology to connect the relationship between the spatial distribution and the electrochemical activity of the HER active sites.

As an electrochemical imaging tool, the combination of scanning probe microscopy and microelectrode is effective to sense the surface reactivity of the catalysis with a micrometer scale. Scanning electrochemical microscopy (SECM<sup>\*2</sup>) has been demonstrated to be one of the powerful tools for determining the relationship between the surface morphology of a sample and its electrochemical activities for screening highly catalytically active sites in catalytic materials.<sup>[3]</sup> However, the spatial resolution of

SECM is the issue for characterizing local electrochemical activity because of the difficulty of the miniaturization of the microelectrode. Scanning electrochemical cell microscopy (SECCM), which uses a nanopipette as a probe in a local and movable electrochemical cell, is an effective tool for operando characterization of surface structures electrochemically in a submicron spatial resolution.<sup>[4]</sup> The advantages of SECCM are that it is a reproducible and reliable technique for fabricating nanoprobes together with fast electrochemical characterization due to its small capacitive current and its ability to prevent sample contamination during scanning.

In this report, the inhomogeneous HER activity on a triangular 1H-MoS<sub>2</sub> monolayer nanosheet, a heterostructures of MoS<sub>2</sub> and WS<sub>2</sub> nanosheets were visualized by using SECCM.<sup>[5]</sup> Our data provides information about the local catalytic properties as well as electrochemical images of the HER current, Tafel slope, and overpotential by measuring the cyclic voltammograms (CVs) at all measurement points during the imaging. These SECCM measurement unveiled heterogeneous reactivity, relationship of layer number and HER activity, and aging effect.

<sup>\*1</sup> Transition-metal dichalcogenides (TMDs) are composed of three atomic planes and often two atomic species: a metal and two chalcogens.

<sup>\*2</sup> SECM uses microelectrode as a probe to detect a oxidation/reduction current on sample surface.

### Scanning electrochemical cell microscopy (SECCM)

The SECCM uses a moveable nanopipette probe containing a 0.5 M H<sub>2</sub>SO<sub>4</sub> solution and a Pd-H<sub>2</sub> quasi-reference counter electrode (QRCE) (Figure 1a). In the case of chloride ion free solutions, Pd-H<sub>2</sub> QRCE was generally used for SECCM experiments. All the potentials were converted into electric potentials when the reversible hydrogen electrode was used for the reference electrode. The following procedure was used to bring the nanopipette towards the sample surface so that the liquid meniscus just made contact at a series of predefined positions, with an electrochemical measurement at each point. First, the nanopipette (meniscus) was withdrawn from its existing position by a specified distance, typically 0.3 μm. Next, the vertical position of the probe was maintained for 60 ms, while the nanopositioning stage moved the specimen to a new imaging point in the xy plane. Then, the nanopipette was lowered at constant fall rate of 7 nm ms<sup>-1</sup> while monitoring the current. Immediately after detecting a current (2 pA threshold) by forming the electrical contact between the nanopipette and the sample through the

nanoipette meniscus, the approach was stopped and the vertical position of the nanopipette was saved along with the x,y co-ordinate to form a topography map. Local cyclic voltammogram was performed by sweeping the applied voltage (scan rate was set at 130-150 V/s, the measurement time was 20 ms/point) after 0.2 ms wait for suppression of capacitive current. After the electrochemical measurement, the nanopipette was quickly withdrawn by the specified distance to start a new measurement cycle. In this way, simultaneous pictures of topography and redox activity were built up.

### HER reactivity mapping on MoS<sub>2</sub> nanosheet

1H-MoS<sub>2</sub> nanosheets were characterized by measuring the cyclic voltammograms (CVs) at all measurement points during the SECCM imaging. CV scan rate was set at 130 V/s, the measurement time was 20 ms/point, and the imaging time (128 × 128 points) was typically 40 min. The current image was obtained by picking up the current signal from CV or applied DC voltage (-1.3 V vs. RHE). An electrode surface area with a radius of 50 nm in the electrochemical cell was used to calculate the current density. The overpotential was evaluated at a 30 mA/cm<sup>2</sup> current density. The CV measurement was done at all of the scanning points, and SECCM provided three electrochemical mapping images of the HER current, Tafel slope, and overpotential, produced simultaneously. SECCM images and a graph of the electrochemical properties of the 1H-MoS<sub>2</sub> nanosheets are shown in Figure 1 (b-d). At the edge region, 1H-MoS<sub>2</sub> nanosheets showed a high current response, a low overpotential, and a low Tafel slope. Notably, it was also observed that there were some activities as a line on the HOPG, which corresponds to the HOPG step edges showing slightly high current responses. In order to characterize the HER catalytic activity of the edge and terrace regions of the 1H-MoS<sub>2</sub> nanosheets, CV curves were selected and averaged from the edge and terrace regions, respectively, shown in Figure 1(e-g). An overpotential with a HER current density at 30 mA/cm<sup>2</sup> and a Tafel slope of 1H-MoS<sub>2</sub> nanosheets edge region, terrace region, and HOPG step are 0.94 V (versus RHE), 1.06 V (versus RHE), and 1.15 V (versus RHE) and 130 mV/dec, 130 mV/dec, and 121 mV/dec, respectively. The relatively larger overpotentials were obtained by the SECCM measurement than typical bulk measurement. In the case of SECCM measurement, the IR drop effect was neglectable because of the small faradaic current. The origin of the overpotentials would be due to the difference of the number of catalytic active sites. These results indicate that the edge region of the 1H-MoS<sub>2</sub> nanosheets show low overpotential but the Tafel slope was not seen remarkable

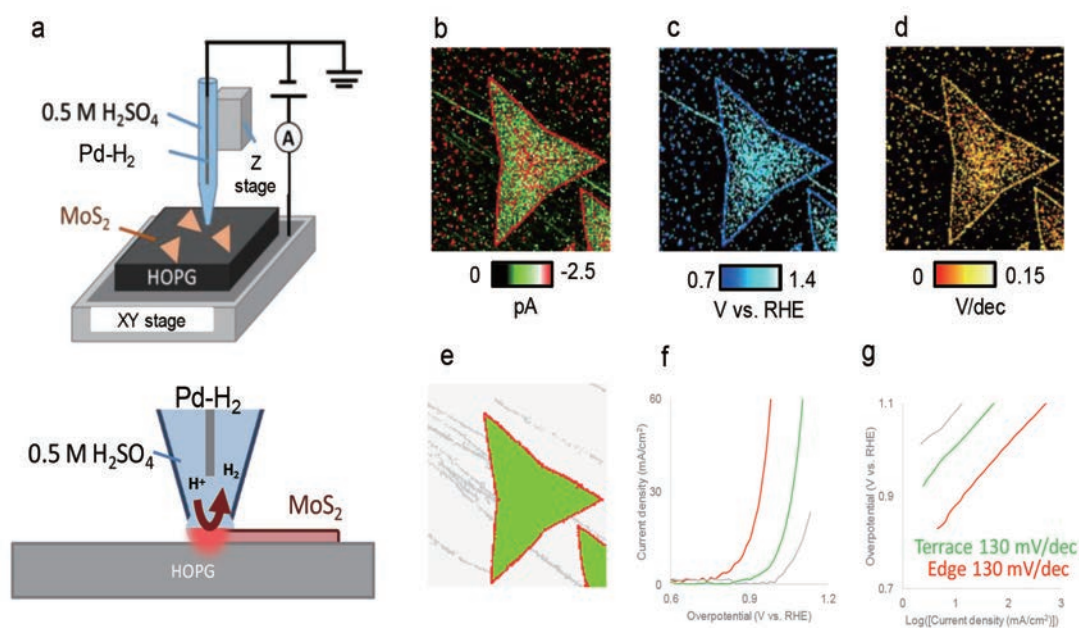


Figure 1 (a) Schematic illustration of SECCM measurements of MoS<sub>2</sub> nanosheets. Pd-H<sub>2</sub> used as a quasi-reference electrode. Nanopipette filled with 0.5 M H<sub>2</sub>SO<sub>4</sub>. SECCM (b) current, (c) overpotential (30 mA/cm<sup>2</sup>), (d) Tafel slope images of 1H MoS<sub>2</sub> nanosheets on HOPG substrate. Scansizes were 15 × 15 μm<sup>2</sup>. Scan rate is 130 V/s. Sweep Voltage were -1.3 V vs. RHE. (e) MoS<sub>2</sub> nanosheets edge(red), terrace(green), and HOPG edge(grey) tricolor images. Graphs showing the (f) overpotential and (g) Tafel slope on the 1H MoS<sub>2</sub> edge (red), terrace (green), and HOPG edge(grey) regions.

difference between edge and terrace region for HER catalysis. The current image shows a three highly active lines contrast at the center, which may correspond to grain boundaries or nanowires in the chemical vapor deposition grown 1H-MoS<sub>2</sub> nanosheets, in addition to the highly active edges.

### Electrochemical activation of MoS<sub>2</sub> nanosheet for enhance the HER activity

The improvement of the HER activity is an important research target for dichalcogenide catalysts. Frank and coworkers recently reported that the electrochemical generation of sulfur vacancies can improve the HER activity.<sup>[6]</sup> Briefly, sulfur vacancies generated by applying a negative potential to MoS<sub>2</sub> are more stable than sulfur on the basal plane. At these sulfur vacancies sites, hydrogen adsorption is thermodynamically favoured than sulfur resorption. Therefore, electrochemically generated sulfur vacancies are stable and work as HER catalytic active sites. We have performed similar experiment using SECCM to improve HER activity at a local area on the MoS<sub>2</sub> nanosheets in order to investigate the position-dependent activation properties. The local SECCM CV imaging of a 1H-MoS<sub>2</sub> nanosheet was performed in three different regions with different scan voltages of -1.10, -1.20, and -1.40 V versus RHE to investigate the relationship between the applied voltage and the activation. After electrochemical activation, CV measurements and imaging were performed over

a large-scale scanning area to capture a whole 1H-MoS<sub>2</sub> nanosheet in order to characterize the local SECCM activation effects. Figure 2(a-c) shows the electrochemical images of the activated 1H-MoS<sub>2</sub> nanosheet. The electrochemically activated area shows a high current response, a low overpotential, and a low Tafel slope. A high HER activity was observed in the area activated by the scan of up to -1.40 V versus RHE, whereas no significant improvement was observed in the HER activity when the scan was reversed at -1.20 V versus RHE. It was also observed that there was SECCM electrochemical treatment induced homogeneous HER activation in the treated area. These results suggest that the electrochemical activation has a threshold voltage (-1.40 vs. RHE) for improving the HER activity. Defect engineering is also a well-known technique that has been used to improve the HER activity of MoS<sub>2</sub>, but its mechanism is unclear. As a demonstration of a defect-engineered sample measurement, we have imaged the HER activity of an over-annealed 1H-MoS<sub>2</sub> nanosheet (300°C in a sulfur atmosphere for 30 min), which had a lot of cracks. Figure 2(d-f) shows the SECCM images of the overannealed 1H-MoS<sub>2</sub> nanosheet. The cracked regions show a low overpotential response and a similar response at their edges. SECCM is also useful for evaluating the treatment effect for improving the catalytic activity of the MoS<sub>2</sub> nanosheet.



## HER activity of the MoS<sub>2</sub> - WS<sub>2</sub> heteronanosheet

Atomic-layer semiconducting heterostructures is an important for tuning the band width.<sup>[7]</sup> However, electrochemical reactivity is closely related to adsorption / dissociation of molecules and electron transfer and Tafel–Volmer reaction is the bottle neck process of HER reaction. To characterize the heterostructures HER activity, we visualized lateral and stacked heterostructure based on MoS<sub>2</sub> and WS<sub>2</sub> heteronanosheet using SECCM and conformed nanosheet topography using AFM (Figure 3(a,b)). The mono or bilayer level lateral and stacked MoS<sub>2</sub> and WS<sub>2</sub>

heteronanosheet structure was clearly visualized by AFM. Specific catalytic ability was not observed at the hetero-junction, but different current signal was obtained on MoS<sub>2</sub> and WS<sub>2</sub> heteronanosheet (Figure 3(c)). To investigate the detail of HER activity difference, we performed high magnification SECCM imaging. The current response is corresponding with the region and clearly categorize the current response of MoS<sub>2</sub> edge (green), WS<sub>2</sub> terrace (red), MoS<sub>2</sub> terrace (blue), and kish graphite terrace (grey).

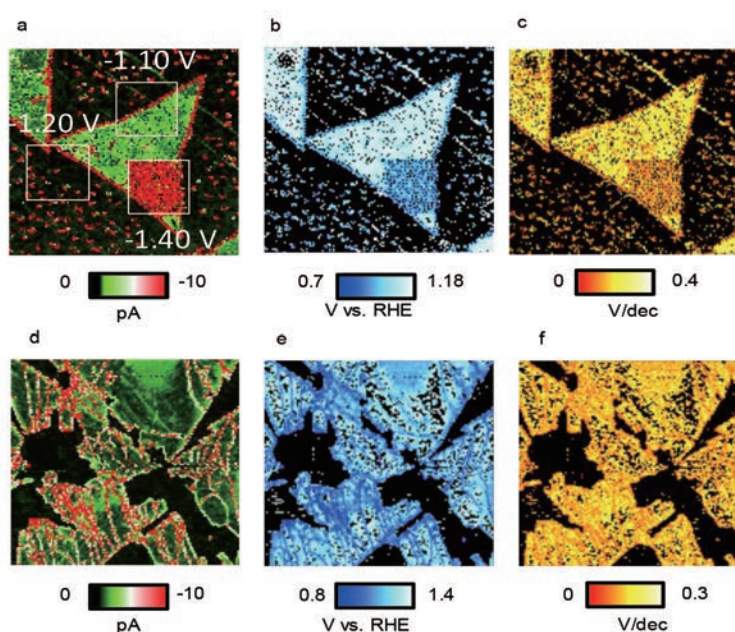


Figure 2 (a) current (b) overpotential (30 mA/cm<sup>2</sup>) and (c) tafel slope images of electrochemical activation and imaging of 1H MoS<sub>2</sub> nanosheets on HOPG substrate. Scansize was 10 × 10 mm<sup>2</sup> and -1.2 V vs. RHE. (d) current (e) overpotential (30 mA/cm<sup>2</sup>) and (f) tafel slope images of heating activated 1H MoS<sub>2</sub> nanosheets on HOPG substrate. Scansize was 10 × 10 mm<sup>2</sup>. -1.1 V vs. RHE.

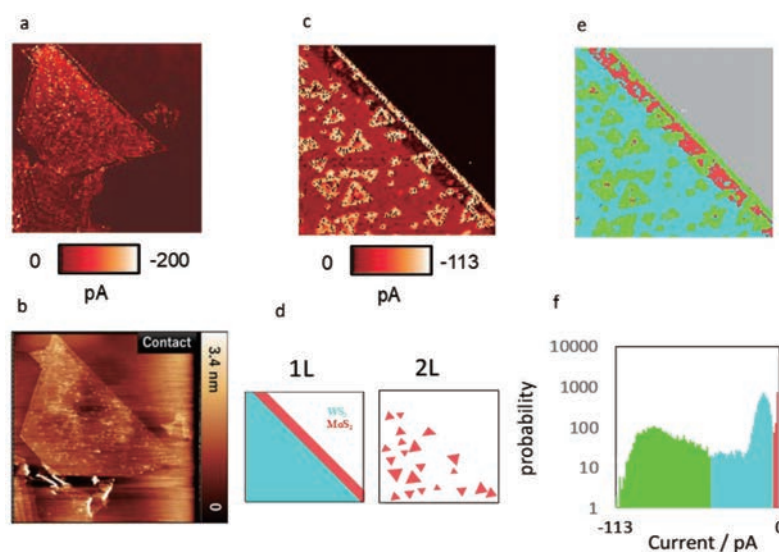


Figure 3 (a) SECCM and (b) AFM images of MoS<sub>2</sub> and WS<sub>2</sub> heteronanosheet on kish graphite. Scansizes were 20 × 20 mm<sup>2</sup> and 18 × 18 mm<sup>2</sup>. Applied voltage was -1.0 V vs. RHE. (c) High magnification SECCM, (d) Schematic illustration, and (e) Four color of MoS<sub>2</sub> and WS<sub>2</sub> heteronanosheet image divided based on current and (f) Data from the SECCM images current plotted as histograms. Scansize was 5 × 5 mm<sup>2</sup> and -1.1 V vs. RHE.

## Characterization of the Layer number related HER activity

The layer number is also reported as an important factor for HER activity because of the electron conductivity related with layer number.<sup>[8]</sup> Therefore, as a next experiment, we characterized the relation of layer number and HER activity. Figure 4(a) shows the multi layered MoS<sub>2</sub> and WS<sub>2</sub> heteronanosheet. To investigate the layer dependent HER activity, we categorized the 1<sup>st</sup> (red), 2<sup>nd</sup> (green), and 3<sup>rd</sup> (grey) layer and characterize the overpotential and Tafel slope. Surprisingly, we could not see clear difference of overpotential (30 mA/cm<sup>2</sup>) and Tafel slope, 0.91 vs. RHE, and 185 mV/dec, at each layer number. (Figure 4 (d, e)). SECCM local electrochemical imaging is important to directly visualizing and characterizing the local catalytic activity without being buried in the average response.

## Characterization of local aging phenomena

Understanding the aging phenomena is very important to use the catalytic material for long time. Nikhil and coworkers reported the aging effect of MoS<sub>2</sub> and WS<sub>2</sub> nanosheets by photoluminescence and XPS.<sup>[9]</sup> They have reported that the origin of the aging of MoS<sub>2</sub> was due to oxidation process of the transition metals at the edge parts

and adsorption of organic contaminants. However, these methods are difficult to characterize the catalytic activity. SECCM can directly visualize the aging effect on transition metal dichalcogenide nanosheet. We characterized HER activity of fresh and partially degraded following room-temperature storage in air for 11 month after the initial synthesis MoS<sub>2</sub> and WS<sub>2</sub> heteronanosheet. The fresh sample shows high activity at the edge. In the case of the pyramid and spiral shape structure WS<sub>2</sub> nanosheets, top regions showed significantly high HER activity (Figure 5(a, b)). On the other hand, edge region of aging sample showed lower current signal compared to terrace region (Figure 5(c)). We also characterize the sample using CV mode SECCM for characterizing overpotential and Tafel slope (Figure 5(d)). The overpotential (30 mA/cm<sup>2</sup>) of edge region (0.91 vs. RHE) was higher than terrace region (0.88 vs. RHE). About the Tafel slope, we could not see significant difference between edge and terrace of MoS<sub>2</sub> and WS<sub>2</sub> heteronanosheet. The degradation of MoS<sub>2</sub> and WS<sub>2</sub> heteronanosheet may be expected to derive from the reaction with oxygen, water, and adsorbed organic contamination. These result mean that characterization of progress of the heterogeneous degradation of HER activity is also important application of SECCM.

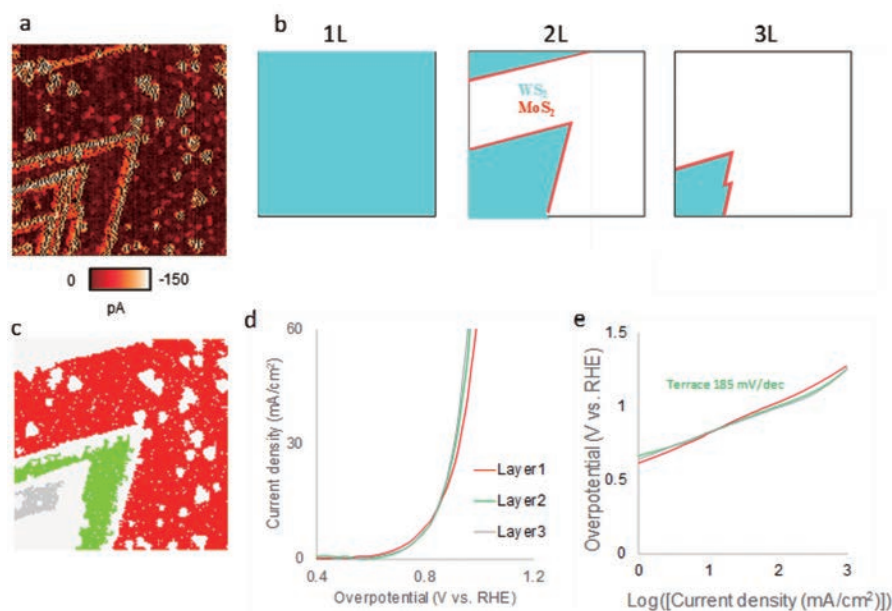


Figure 4 (a) SECCM and (b) Schematic illustration and (c) tricolor images of 1<sup>st</sup> (red), 2<sup>nd</sup> (green), 3<sup>rd</sup> (grey) of MoS<sub>2</sub> and WS<sub>2</sub> heteronanosheet on kish graphite. Scansize was 6 × 6 mm<sup>2</sup> and -1.0 V vs. RHE. Graphs showing the (d) overpotential and (e) Tafel slope of the 1<sup>st</sup> (red), 2<sup>nd</sup> (green), 3<sup>rd</sup> (grey) regions.

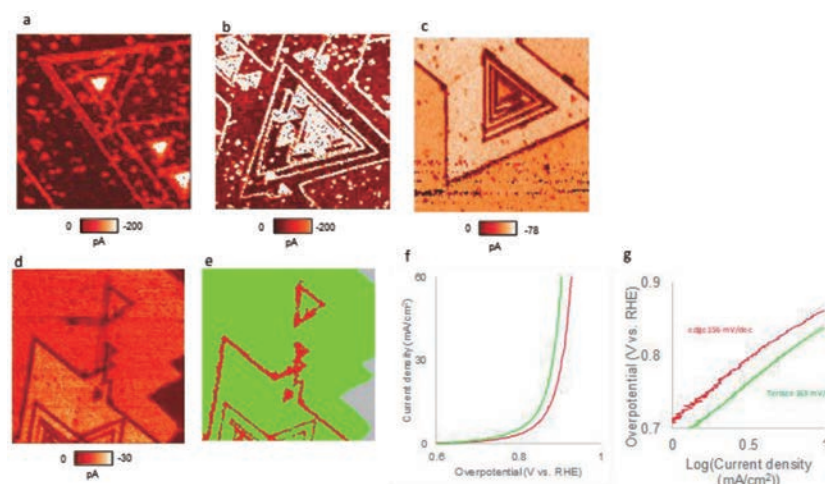


Figure 5 SECCM images of (a, b) fresh and (c) aging MoS<sub>2</sub> and WS<sub>2</sub> heteronanosheet on kish graphite. Scansize were (a) 8 × 8 mm<sup>2</sup> and (b-e) 10 × 10 mm<sup>2</sup>, respectively. Applied voltage were -0.4 V vs. RHE and -0.9 V vs. RHE, respectively. SECCM (d) current imaging of the aging MoS<sub>2</sub> and WS<sub>2</sub> heteronanosheet and (e) tricolor images of edge (red), terrace (green), and HOPG terrace. Scansize was 7 × 7 mm<sup>2</sup> and -0.4 V vs. RHE and -0.9 V vs. RHE. Graphs showing the (f) overpotential and (g) Tafel slope of the aging MoS<sub>2</sub> and WS<sub>2</sub> heteronanosheet edge (red) and terrace (green) regions.

## Conclusion

We have developed SECCM for visualizing HER catalytically active sites in real-space on MoS<sub>2</sub> nanosheets by measuring the distributions of the current, overpotential, and Tafel slope with a submicroscale spatial resolution. The visualization of the HER active sites provides solid experimental evidence to support the previous theoretical prediction and assumption that there is an inhomogeneous catalytic activity between the edges and terraces of 1H-MoS<sub>2</sub> nanosheets. Moreover, the high spatial resolution of SECCM reveals an inhomogeneous HER activity from grain boundaries, small nanosheets, and electrochemically activated regions, which indicates that the HER catalysis of MoS<sub>2</sub> nanosheets may be improved by structure engineering. This study also demonstrates that SECCM is a powerful tool for evaluating the local HER activity for designing the suitable catalytic active structure, phase and can be widely applied for the characterization of 2D catalytic materials.

## References

- [1] Jaramillo, T. F.; Jorgensen, K. P.; Bonde, J.; Nielsen, J. H.; Horch, S.; Chorkendorff, I. Identification of active edge sites for electrochemical H<sub>2</sub> evolution from MoS<sub>2</sub> nanocatalysts. *Science* **2007**, *317* (5834), 100-102. DOI: 10.1126/science.1141483.
- [2] Li, H.; Tsai, C.; Koh, A. L.; Cai, L. L.; Contryman, A. W.; Fragapane, A. H.; Zhao, J. H.; Han, H. S.; Manoharan, H. C.; Abild-Pedersen, F.; et al. Activating and optimizing MoS<sub>2</sub> basal planes for hydrogen evolution through the formation of strained sulphur vacancies (vol 15, pg 48, 2016). *Nat Mater* **2016**, *15* (3). DOI: 10.1038/NMAT4564.
- [3] Fernandez, J. L.; Walsh, D. A.; Bard, A. J. Thermodynamic guidelines for the design of bimetallic catalysts for oxygen electroreduction and rapid screening by scanning electrochemical microscopy. M-Co (M : Pd, Ag, Au). *Journal of the American Chemical Society* **2005**, *127* (1), 357-365. DOI: 10.1021/ja0449729.
- [4] Takahashi, Y.; Kumatani, A.; Munakata, H.; Inomata, H.; Ito, K.; Ino, K.; Shiku, H.; Unwin, P. R.; Korchev, Y. E.; Kanamura, K.; et al. Nanoscale visualization of redox activity at lithium-ion battery cathodes. *Nature communications* **2014**, *5*, 5450. DOI: Artn 5450. DOI: 10.1038/Ncomms6450.
- [5] Takahashi, Y.; Kobayashi, Y.; Wang, Z.; Ito, Y.; Ota, M.; Ida, H.; Kumatani, A.; Miyazawa, K.; Fujita, T.; Shiku, H.; et al. High-Resolution Electrochemical Mapping of the Hydrogen Evolution Reaction on Transition-Metal Dichalcogenide Nanosheets. *Angewandte Chemie* **2020**, *59* (9), 3601-3608. DOI: 10.1002/anie.201912863 From NLM PubMed-not-MEDLINE.
- [6] Tsai, C.; Li, H.; Park, S.; Park, J.; Han, H. S.; Nørskov, J. K.; Zheng, X.; Abild-Pedersen, F. Electrochemical generation of sulfur vacancies in the basal plane of MoS<sub>2</sub> for hydrogen evolution. *Nature communications* **2017**, *8*, 15113. DOI: 10.1038/ncomms15113.
- [7] Kobayashi, Y.; Yoshida, S.; Maruyama, M.; Mogi, H.; Murase, K.; Maniwa, Y.; Takeuchi, O.; Okada, S.; Shigekawa, H.; Miyata, Y. Continuous Heteroepitaxy of Two-Dimensional Heterostructures Based on Layered Chalcogenides. *Acs Nano* **2019**, *13* (7), 7527-7535. DOI: 10.1021/acsnano.8b07991.
- [8] Yu, Y. F.; Huang, S. Y.; Li, Y. P.; Steinmann, S. N.; Yang, W. T.; Cao, L. Y. Layer-Dependent Electrocatalysis of MoS<sub>2</sub> for Hydrogen Evolution. *Nano Lett* **2014**, *14* (2), 553-558. DOI: 10.1021/nl403620g.
- [9] Gao, J.; Li, B.; Tan, J.; Chow, P.; Lu, T.-M.; Koratkar, N. Aging of Transition Metal Dichalcogenide Monolayers. *Acs Nano* **2016**, *10* (2), 2628-2635. DOI: 10.1021/acsnano.5b07677.
- [10] Chen, L.; Liu, B. L.; Abbas, A. N.; Ma, Y. Q.; Fang, X.; Liu, Y. H.; Zhou, C. W. Screw-Dislocation-Driven Growth of Two-Dimensional Few-Layer and Pyramid-like WSe<sub>2</sub> by Sulfur-Assisted Chemical Vapor Deposition. *Acs Nano* **2014**, *8* (11), 11543-11551. DOI: 10.1021/nn504775t.
- [11] Fan, X. P.; Jiang, Y.; Zhuang, X. J.; Liu, H. J.; Xu, T.; Zheng, W. H.; Fan, P.; Li, H. L.; Wu, X. P.; Zhu, X. L.; et al. Broken Symmetry Induced Strong Nonlinear Optical Effects in Spiral WS<sub>2</sub> Nanosheets. *Acs Nano* **2017**, *11* (5), 4892-4898. DOI: 10.1021/acsnano.7b01457.



Dr. TAKAHASHI Yasufumi

高橋 康史

Professor,  
Department of Electronics,  
Graduate School of Engineering,  
Nagoya University